Nonequilibrium weak processes in kaon condensation. II. Kinetics of condensation

Takumi Muto*

Department of Physics, Chiba Institute of Technology, 2-1-1 Shibazono, Narashino, Chiba 275-0023, Japan

Toshitaka Tatsumi†

Department of Physics, Kyoto University, Kyoto 606-8502, Japan

Naoki Iwamoto‡

Department of Physics and Astronomy, The University of Toledo, Toledo, Ohio 43606-3390

(Received 20 September 1999; published 22 March 2000)

The kinetics of negatively charged kaon condensation in the early stages of a newly born neutron star is considered. The thermal kaon process, in which kaons are thermally produced by nucleon-nucleon collisions, is found to be dominant throughout the equilibration process. Temporal changes of the order parameter of the condensate and the number densities of the chemical species are obtained from the rate equations, which include the thermal kaon reactions as well as the kaon-induced Urca and the modified Urca reactions. It is shown that the dynamical evolution of the condensate is characterized by three stages: the first, prior to establishment of a condensate, the second, during the growth and subsequent saturation of the condensate, and the third, near chemical equilibrium. The connection between the existence of a soft kaon mode and the instability of the noncondensed state is discussed. Implications of the nonequilibrium process on the possible delayed collapse of a protoneutron star are also mentioned.

PACS number(s): 26.60.+c, 05.30.Jp, 13.75.Jz, 82.20.Mj

I. INTRODUCTION

The possibility that baryonic matter may undergo a transition to a new hadronic phase consisting of a condensate of negatively charged kaons (K^-) in high density matter has been extensively discussed [1–6]. The kaon condensation may be formulated on the basis of $SU(3)_L \times SU(3)_R$ current algebra and partial conservation of axial vector current in a model-independent way [2,3]. Within this framework, the s-wave kaon-condensed state $|\theta\rangle$ is generated by a chiral rotation of the normal state $|\text{normal}\rangle$ as $|\theta\rangle = \hat{U}_K |\text{normal}\rangle$, where $\hat{U}_K = \exp(i\mu_K t \hat{Q}) \exp(i\theta \hat{Q}_4^5)$ is a unitary operator. Here μ_K is the kaon chemical potential, θ the chiral angle, which is the order parameter of the condensate, and $\hat{Q}$ ($\hat{Q}_4^5$) is the electromagnetic charge operator (the axial charge operator). The classical K^- field is then written as $\langle K^- \rangle \equiv \langle \theta | K^- | \theta \rangle = (f/\sqrt{2}) \sin\theta \exp(-i\mu_K t)$ with $f (=93 \text{ MeV})$ the meson decay constant.

Kaon condensation is a form of Bose-Einstein condensation (BEC): the lowest excitation energy of the K^- decreases in a nuclear medium with an increase in the baryon number density due to an attractive s-wave kaon-nucleon (KN) interaction. When the lowest excitation energy becomes equal to the charge chemical potential, the distribution function for the K^- diverges and a macroscopic number of kaons appear. The relevant s-wave KN interaction comes mainly from the scalar interaction (the KN sigma term, Σ_{KN}) and the vector interaction (the Tomozawa-Weinberg term) [2–4].

The baryon number density for the onset of kaon condensation in stable neutron-star matter has been predicted to be 3–4 times the nuclear matter density n_0 ($=0.16 \text{ fm}^{-3}$), depending on the magnitude of Σ_{KN}. Motivated by studies of kaon condensation, the in-medium KN interaction has recently been elaborated both theoretically and experimentally, through KN scattering [7–9], kaonic atoms [10], and kaon-antikaon production via relativistic nucleus-nucleus collisions [11–15]. The experimental results suggest a substantial decrease in the antikaon effective mass, which in turn favors the possible existence of a kaon condensate in the core of a neutron star.[1]

The appearance of the kaon-condensed phase in a neutron star would lead to softening of the equation of state (EOS) [3,12,17] and also accelerate cooling of neutron stars via enhanced neutrino emission which is given by weak processes in kaon condensation [17–21]. The softening of the EOS associated with kaon condensation has been used to construct a model in which the collapse of a hot protoneutron star to a black hole is delayed [22–24];[2] initially, there is no

---

*Email address: muto@pf.it-chiba.ac.jp

†Email address: tatsumi@ruby.scphys.kyoto-u.ac.jp

‡Email address: iwamoto@uoft02.utoledo.edu

[1]Recently, the antikaon potential at high momenta or temperature has been considered with reference to subthreshold antikaon production in heavy-ion collisions [16]. It has been shown that the optical potential becomes repulsive at high momentum or high temperature. On the other hand, the in-medium production cross section of antikaons is enhanced via pions and Σ hyperons. It would be important in future study to take into account the finite momentum and temperature effects on the in-medium kaon self-energy and to see how the in-medium cross section of the antikaon production is relevant to the nonequilibrium process in kaon condensation in neutron stars.

[2]Similar delayed collapse mechanisms of a hot protoneutron star to a more compact neutron star or to a black hole, attributed to other hadronic phase transitions [5,25–29] or a transition to a strange matter [30,31], have been considered by some authors.

kaon condensation in protoneutron stars, since the neutrino degeneracy and thermal effects raise the threshold density for kaon condensation [32]. A kaon condensate is formed during the evolution into a compact neutron star through deleptonization and cooling. The maximum mass of the kaon-condensed neutron star is estimated to be ~ 1.5 $M_\odot$ with $M_\odot$ the solar mass [3,12,17], which is smaller than the maximum mass of ordinary neutron stars ($\sim 2.0 M_\odot$) [33] because of the significant softening of the EOS due to the appearance of the condensates. If the mass of a protoneutron star after deleptonization or cooling exceeds the maximum mass of the kaon-condensed neutron star, the star eventually collapses to a black hole. Such a scenario for the formation of a low-mass black hole (1.5–2.0 $M_\odot$) has been presented by Brown and Bethe [22] to interpret the absence of a pulsar signature in SN 1987A [34]. Following their scenario, Baumgarte *et al.* [23] made a numerical simulation for the delayed collapse of a protoneutron star by the use of an EOS including the phase transition to the kaon-condensed phase [23].

In these studies, the equilibrated EOS with kaon condensation was used. The kaons are created through *weak interactions* that change strangeness during the appearance and the growth of the condensate, and the time scale for the weak reactions are much larger than those for the strong and electromagnetic reactions which are responsible for the thermal equilibration of the system.[3] In addition, there are at least three time scales which characterize the dynamical evolution of a newly born neutron star: the time scale for gravitational collapse (of order of a millisecond) and those for deleptonization and initial cooling (of order of ten seconds). If the weak reactions which are responsible for the formation of a condensate proceed on a longer time scale than these time scales, they may control the dynamical evolution of a neutron star just after a supernova explosion. In this case, the nonequilibrium processes in kaon condensation which are brought about by the weak reactions must be considered.

The time evolution of the system is determined by the Hamiltonian,

$$\hat{H} = \hat{H}_{\text{strong}} + \hat{H}_{\text{weak}}, \tag{1}$$

with the strong (weak) Hamiltonian $\hat{H}_{\text{strong}}$ ($\hat{H}_{\text{weak}}$). In our case the state $|\theta(t),t\rangle$ is specified by the parameters, θ, μ_n (μ_p) the neutron chemical potential (the proton chemical potential), μ_K, and μ_e the electron chemical potential, for given temperature T and baryon number density n_B. Alternatively we may choose another set of operators, $\hat{\theta}$, the number densities $\hat{n}_i$ ($i = p, n, K, e$) to specify the state. If the weak Hamiltonian $\hat{H}_{\text{weak}}$ is negligibly small, then the time scale of the weak interaction is very large ($\tau_{\text{weak}} \gg \tau_{\text{strong}}$). In such a case, it is obvious that all the number densities are time independent, $\dot{\hat{n}}_i = 0$, which in turn implies $\dot{\hat{\theta}} = 0$, or they

can commute with $\hat{H}_{\text{strong}}$, $[\hat{n}_i, \hat{H}_{\text{strong}}] = 0$, due to baryon number, strangeness, charge and lepton number conservations. Thus we can find the simultaneous eigenstate of $\hat{H}_{\text{strong}}$ and $\hat{n}_i$. Hence, if we apply the adiabatic (Born-Oppenheimer) approximation, then the time dependence of $n_i(t) \equiv \langle \theta(t),t | \hat{n}_i | \theta(t),t \rangle$ is determined by the weak interaction Hamiltonian $\hat{H}_{\text{weak}}$, which leads to the rate equations. With $n_i(t)$ taken to be a function of time, it is possible to fix the time and construct an instantaneous eigenstate of $\hat{H}_{\text{strong}}$ and $\hat{\theta}$, by considering the extremum conditions for the thermodynamic potential Ω given only by the strong interaction Hamiltonian $\hat{H}_{\text{strong}}$,

$$|\theta(t),t\rangle \simeq |\theta(t), n_K(t), n_n(t), n_p(t), n_e(t)\rangle. \tag{2}$$

Solving the rate equations then allows the temporal change of n_i to be determined, while the time dependence of the order parameter θ is determined by use of the thermodynamic potential Ω.

The nonequilibrium processes in the kaon-condensed state $|\theta(t),t\rangle$ have been previously investigated in [35], with account taken of both the kaon-induced Urca process and the modified Urca process. The former process (abbreviated to KU-F and KU-B, where F and B stand for forward and backward reactions, respectively) is represented by the reactions

$$n(p) \rightarrow n(p) + e^- + \bar{\nu}_e, \tag{3a}$$

$$n(p) + e^- \rightarrow n(p) + \nu_e, \tag{3b}$$

and provides the most efficient cooling mechanism for the star via neutrino and antineutrino emissions [18,19]. In terms of the condensate $\langle K^- \rangle$, by which the system is supplied with energy and the reactions become kinematically possible, the KU process (3) can be written symbolically as $n(p) + \langle K^- \rangle \rightarrow n(p) + e^- + \bar{\nu}_e$, $n(p) + e^- \rightarrow n(p) + \langle K^- \rangle + \nu_e$. The modified Urca process (MU-F and MU-B) [36,37], represented by the reactions

$$n + n \rightarrow n + p + e^- + \bar{\nu}_e, \tag{4a}$$

$$n + p + e^- \rightarrow n + n + \nu_e, \tag{4b}$$

is a standard cooling process for a normal neutron star. It is to be noted that the direct Urca process (DU), $n \rightarrow p + e^- + \bar{\nu}_e$, $p + e^- \rightarrow n + \nu_e$, becomes possible in the normal phase [38,39] if the proton fraction is large enough and that it dominates over the MU reaction. The DU reaction is further assisted in the presence of a kaon condensate [17,21]. However, the onset density for DU depends on the density dependence of the symmetry energy $E_{\text{sym}}(n_B)$, which has an ambiguity depending on the EOS [21,39]. We have also checked that even if the DU reaction is incorporated in the equilibration process, the main results in this paper are not altered except for the asymptotic behavior near chemical equilibrium. Hence, throughout this paper, we do not take into account the DU reaction in the normal phase or in the kaon-condensed phase. Further, we do not take into account

---

[3] In Ref. [17], a discussion was made on the weak processes, $n \leftrightarrow p + K^-$, $e^- \leftrightarrow K^- + \nu_e$, in relation to the formation of a kaon condensate.

the hyperon degrees of freedom, so that we omit the weak reactions associated with hyperons [40], taking the same standpoint as in Paper I.

Because the transition matrix element for KU is proportional to $\sin\theta$, this process is operative only in the presence of a condensate. Thus, spontaneous creation of a condensate from the noncondensed state cannot occur solely by way of the KU and MU reactions, and, for this reason in Ref. [35], a small seed of the condensate ($\theta \neq 0$) was put in by hand.

In the noncondensed state, kaons are produced thermally by the weak reactions

$$n+n \rightarrow n+p+K^-, \tag{5a}$$

$$n+p+K^- \rightarrow n+n, \tag{5b}$$

where a spectator neutron must take part in the reactions such that the kinematical condition in a degenerate Fermi system is satisfied.[4] The thermal kaons are then converted to a condensate. Thus we can discuss the onset and the growth of a kaon condensate consistently without any *ad hoc* seed (see Sec. III), in which case the process (5) is primarily responsible for the onset of condensation. It is to be noted that net strangeness is not changed via strong reactions, e.g., the kaon-antikaon production $NN \rightarrow NNK^+K^-$, while the time scales for the creation of the antikaons via strong reactions are very short as compared with the weak reactions. The effects of these strong reactions on the kinetics of condensation are taken into account only implicitly through the assumption that the system is in thermal equilibrium. Thus, it is the weak reactions that determine the time scales for the appearance of a seed with net strangeness and its growth. We will refer to the reaction (5) as the thermal kaon process, and abbreviate them to KT-F and KT-B, respectively.

In a previous paper [46] (Paper I), we have obtained the reaction rate for KT, and discussed the effects of thermal kaons on the KT reaction rate in both the noncondensed and condensed states. We have also compared the KT reaction rate with the rates for the KU and MU reactions and obtained the following results: (i) In the noncondensed state, where the system is far from chemical equilibrium, hard thermal kaons with large momenta make the major contribution to the KT reaction rate, whereas in the condensed state, the soft thermal kaons, which appear as a Goldstone mode from the spontaneous breaking of *V*-spin symmetry [47], contribute significantly to the KT reaction rate. (ii) The KT reaction rate is larger than the rates for the KU and MU reactions over the

_____

[4]It is to be noted that hyperons may appear in neutron stars at 2–3 n_0 [41–45] and that they also soften the EOS. Some authors discussed a delayed collapse of protoneutron stars based on the EOS with a transition of supernova matter to a hyperonic matter [27–29]. If the hyperons exist, other weak reactions such as the nonmesic decay of the hyperons, $NN \rightarrow \Lambda N$, could be relevant to the nonequilibrium process. The onset density of hyperons in a neutron star depends on the hyperon-nucleon and hyperon-hyperon interactions which remain to be explored further from both theoretically and experimentally.

relevant temperatures and baryon number densities. (iii) The KT process is dominant in the kaon-condensed state in chemical equilibrium as well as in the noncondensed state, and may determine the evolution of the system.

Based on the above results for the KT reactions, we in this paper, investigate the nonequilibrium weak processes in kaon condensation by taking into account the KT process as well as the KU and MU processes, and clarify the effects of thermal kaons on the kinetics of condensation. Assuming that the system is in thermal equilibrium, we solve the rate equations given by the relevant weak reactions (3)–(5), and discuss the temporal behavior of the number densities of the chemical species, the order parameter of the condensate, and other physical quantities. In general, the energy, produced in the course of the nonequilibrium process, is dissipated into the surroundings, resulting in a rise in the temperature of the system. For simplicity, however, the temperature is kept constant throughout this paper. We find two characteristic time scales for the onset of a condensate and its subsequent growth. The magnitudes of these time scales are compared with other time scales characterizing the collapse of a newly born neutron star, and possible effects on stellar collapse are discussed.

The paper is organized as follows: The description of the nonequilibrium state based on the thermodynamic potential is addressed in Sec. II, and the formulation for obtaining the rate equations is given in Sec. III. The numerical results are then presented in Sec. IV, and summary and concluding remarks are given in Sec. V. In the Appendix, an asymptotic behavior of the system near chemical equilibrium is discussed. Specifically, an expression for the relaxation time near chemical equilibrium is derived analytically.

II. DESCRIPTION OF THE NONEQUILIBRIUM STATE

A. Thermodynamic potential

Here we define the physical conditions for a nonequilibrium kaon-condensed state, $|\theta(t),t\rangle$.[5] The system is described by a thermodynamic potential Ω. The microscopic quantities, such as the excitation energies of the baryons and the thermal and condensed kaons, are determined by the strong and electromagnetic interactions among the kaons, baryons and leptons. The time scales for these interactions are much smaller than those for weak reactions. Therefore, in setting up the kinetic equations, that determine the relatively slow change of chemical composition via weak reactions, the system may be assumed to be in thermal equilibrium, maintained by much faster strong and electromagnetic reactions. As a consequence, the physical quantities for the nonequilibrium state evolve adiabatically, adjusting to the gradual change of the chemical composition brought about by the weak processes.

Assuming thermal equilibrium, we adopt the thermodynamic potential Ω of the kaon-condensed phase which was derived by Tatsumi and Yasuhira from chiral symmetry [47],

_____

[5]We use the units in which $\hbar = c = k_B = 1$ throughout this paper.

including the thermal and quantum fluctuations around a condensate. In the present work, we shall neglect, for the sake of simplicity, both zero-point and thermal fluctuations in the thermodynamic variables except for the thermal contribution to the kaon number density, which allows us to see the effects of thermal kaons on the kinetics of condensation. Thus our expression for Ω corresponds to the heavy-baryon limit for the nucleons [47]. With these assumptions, the thermodynamic potential per unit volume Ω/V of the kaon-condensed phase is written as

$$\Omega/V=(\Omega_C+\Omega_K+\Omega_N+\Omega_e)/V, \qquad (6)$$

where Ω_C and Ω_K are the potentials arising from a condensate and thermal fluctuations for the kaons, respectively, and Ω_N and Ω_e are the corresponding potentials for the nucleons and the electrons, respectively. Here, Ω, the number density n_i and the chemical potential μ_i $(i=p,n,e^-,K)$ are related to each other by $n_i=-\partial(\Omega/V)/\partial\mu_i$. Specifically, the classical contribution from the condensate, Ω_C, is given by

$$\Omega_C/V=f^2m_K^2(1-\cos\theta)-\frac{1}{2}f^2\mu_K^2\sin^2\theta, \qquad (7)$$

where m_K is the free kaon mass ($=494$ MeV). In contrast, the thermal kaon contribution, Ω_K, is given by

$$\Omega_K/V=T\int\frac{d^3p_K}{(2\pi)^3}\ln(1-e^{-[\omega_+(\mathbf{p}_K)+\mu_K]/T})$$
$$\times(1-e^{-[\omega_-(\mathbf{p}_K)-\mu_K]/T}), \qquad (8)$$

with $\omega_+(\mathbf{p}_K)$ $[\omega_-(\mathbf{p}_K)]$ the excitation energy for K^+ (K^-) [cf. Sec. II B for the explicit expressions for $\omega_\pm(\mathbf{p}_K)$], and the nucleon contribution Ω_N is written in the standard form:

$$\Omega_N/V=\mathcal{E}_N-\mu_pn_p-\mu_nn_n \qquad (9)$$

where the energy density for the nucleons is given by

$$\mathcal{E}_N=\frac{3}{5}\frac{(3\pi^2)^{2/3}}{2m_N}(n_p^{5/3}+n_n^{5/3})-f^2(\sigma+2b\mu_K)(1-\cos\theta)$$
$$+V_{\text{sym}}(n_B)(n_p-n_n)^2/n_B. \qquad (10)$$

The first term in the right-hand side (rhs) of Eq. (10) is the nucleon Fermi-gas energy density, with m_N the nucleon mass, and the quantity σ in the second term defined as $\sigma\equiv n_B\Sigma_{KN}/f^2$, and $b\equiv(n_p+\frac{1}{2}n_n)/(2f^2)$ is the V-spin density (see Sec. IV A for specific values). The terms involving σ and b, respectively, come from the s-wave K^-N interaction given by the KN sigma term and the Tomozawa-Weinberg term. The expression for the energy contribution from kaon-kaon and kaon-nucleon interactions is essentially determined in a model-independent way by chiral symmetry. The third term in Eq. (10) is the potential energy contribution to the symmetry energy. For $V_{\text{sym}}(n_B)$, we use the expression given by Prakash *et al.* [48]:

$$V_{\text{sym}}(n_B)=\left[S_0-(2^{2/3}-1)\frac{3}{5}\epsilon_{F,0}\right]F(n_B), \qquad (11)$$

where S_0 ($=30$ MeV) is the empirical symmetry energy, and $\epsilon_{F,0}$ is the Fermi energy in the symmetric nuclear matter at the density n_0, with the function $F(n_B)$ taken as $F(n_B)=n_B/n_0$ for simplicity. The chemical potentials for the proton and the neutron (respectively) in Eq. (9) are given by $\mu_p=\partial\mathcal{E}_N/\partial n_p$ and $\mu_n=\partial\mathcal{E}_N/\partial n_n$, respectively, so that the difference between μ_p and μ_n in the condensed state is written as

$$\mu_p-\mu_n=\frac{(3\pi^2n_p)^{2/3}}{2m_N}-\frac{(3\pi^2n_n)^{2/3}}{2m_N}$$
$$+4V_{\text{sym}}(n_B)\cdot(n_p-n_n)/n_B-\frac{1}{2}\mu_K(1-\cos\theta).$$
$$(12)$$

For Ω_e, we use the ultrarelativistic form for electrons,

$$\Omega_e/V=\frac{\mu_e^4}{4\pi^2}-\mu_en_e=-\frac{\mu_e^4}{12\pi^2}, \qquad (13)$$

where μ_e is the electron chemical potential and n_e $[=\mu_e^3/(3\pi^2)]$ is the electron number density. Note that $\mu_e\neq\mu_K$ when the system is not in chemical equilibrium.

B. Thermal kaon excitation

As can be seen in Eq. (6), only the thermal kaon excitations constitute the thermal fluctuations in the thermodynamic potential Ω, because they are responsible for the formation of a condensate through the weak reactions KT [(5)]. The excitation energy for the thermal kaons, $\omega_\pm(\mathbf{p}_K)$, appearing in Ω_K [Eq. (8)], is obtained from the dispersion relations for kaon modes in the condensed state. The expression for $\omega_\pm(\mathbf{p}_K)$ depends on the method for treating the fluctuations around the condensate [47,49], but numerical results have shown that there is little difference between the two methods used in Refs. [47] and [49]. Later on we use the result of Ref. [47]:

$$\omega_\pm(\mathbf{p}_K)\simeq\pm\{b+\mu_K(\cos\theta-1)\}+[\mathbf{p}_K^2+(b^2+\widetilde{m_K^{*2}})]^{1/2}, \qquad (14)$$

where $\widetilde{m_K^{*2}}\equiv m_K^{*2}\cos\theta=(m_K^2-\sigma)\cos\theta$, and m_K^* denotes the effective kaon mass which is reduced due to the KN scalar interaction Σ_{KN} [3]. Using Eq. (14) one obtains the total kaon number density from the relation, $n_K=-\partial(\Omega/V)/\partial\mu_K$:

$$n_K=\zeta_K+n_K^T. \qquad (15)$$

Here ζ_K is the condensed part of the kaon number density:

$$\zeta_K\equiv-\partial(\Omega_C/V+\Omega_N/V)/\partial\mu_K$$
$$=\mu_Kf^2\sin^2\theta+2bf^2(1-\cos\theta), \qquad (16)$$

and n_K^T is the thermal part:

$$n_K^T = -\partial(\Omega_K/V)/\partial\mu_K$$

$$= \frac{1}{(2\pi)^3}\cos\theta\int d^3p_K f_K(\mathbf{p}_K) \qquad (17)$$

with

$$f_K(\mathbf{p}_K) = \frac{1}{e^{[\omega_-(\mathbf{p}_K)-\mu_K]/T}-1} - \frac{1}{e^{[\omega_+(\mathbf{p}_K)+\mu_K]/T}-1},$$

$$(18)$$

where the first and second terms are the Bose-Einstein distribution functions for the K^- and K^+ mesons, respectively. It is to be noted that the expression (17) is slightly different from the usual one for the noncondensed state by a reduction factor $\cos\theta$ due to the existence of the condensate. Expression (16) is equivalent to the strangeness number density $\zeta_K = \langle K^-|\hat{S}|K^-\rangle$ with the strangeness operator $\hat{S} \equiv 2(\hat{Q}-\hat{I}_3 -\hat{B})$.

By the use of the classical field equation for θ, $\partial\Omega/\partial\theta = 0$ [3,47],

$$\sin\theta(\mu_K^2\cos\theta + 2b\mu_K - m_K^{*2}) = 0, \qquad (19)$$

which is valid where fluctuations of kaons can be neglected [47], it can be seen from Eq. (14) that, in the condensed phase ($\theta \neq 0$), the lowest excitation energy of K^- is equal to the kaon chemical potential, i.e., $\omega_-(\mathbf{p}_K=0) = \mu_K$. This soft mode results from the spontaneous V-spin symmetry breaking in the condensed phase (Goldstone mode), and leads to a divergence of $f_K(\mathbf{p}_K)$ at $\mathbf{p}_K=0$ in the condensed state. On the other hand, in the limit $\theta=0$ in Eq. (14), one obtains the excitation energy of kaons in the normal (noncondensed) phase:

$$\omega_\pm(\mathbf{p}_K) = \pm b + [\mathbf{p}_K^2 + (b^2 + m_K^{*2})]^{1/2}. \qquad (20)$$

In this case, there is a gap between the lowest excitation energy $\omega_-(\mathbf{p}_K=0)$ and μ_K, so that $f_K(\mathbf{p}_K)$ has no singularity. The appearance of a soft kaon mode is also related to an instability of the normal state with respect to the onset of a condensate. (See also Sec. IV A.)

III. KINETICS OF CONDENSATION

A. Rate equations

The thermally excited kaons, which are produced via the weak reactions KT, are converted into a condensate through kaon-nucleon and kaon-kaon scatterings: $KN \rightarrow \langle K\rangle N$, $KK \rightarrow K\langle K\rangle$. The time required for the conversion of the thermal kaons to a condensate through strong interaction collisions is negligible compared with the time scale governed by the weak reactions. This is consistent with the assumption that the system is in *thermal equilibrium*, as discussed in Sec. II A. Thus, we put aside the detailed conversion mechanisms of the thermal kaons into a condensate, and study the kinetics of condensation due to the weak reactions to obtain the typi-

cal time scales for the development of a condensate. With the kaon number density given by Eq. (15), one can see that the condensate appears spontaneously once the number density of the thermal kaons is saturated for a given temperature. With this simplification, we can describe the growth of the condensate during the whole nonequilibrium stage by following the kinetics of the condensate semiclassically, avoiding the discussion of quantum nucleation of the condensates.[6]

In general, the heat released by dissipation of energy in the system is expected to increase the temperature T. The temporal change of the temperature, $T(t)$ can be obtained from the equation that gives the rate of change of the internal energy of the system: e.g.,

$$\partial E/\partial t = -\epsilon_\nu - \epsilon_{\bar{\nu}} \qquad (21)$$

with ϵ_ν, $\epsilon_{\bar{\nu}}$ the luminosities of neutrinos and antineutrinos, respectively, for the neutrino-free-streaming case. For simplicity, however, we take the temperature to be constant during the nonequilibrium process. A more realistic calculation including the variation of the temperature will be discussed in the future.

The number density of each chemical species is determined by the rate equations, with the rates of change of the electron (n_e), the kaon (n_K), and the proton (n_p) number densities given by

$$dn_e(t)/dt = \Gamma^{(\text{KU-F})}(\xi^{(\text{KU})}(t),T) - \Gamma^{(\text{KU-B})}(\xi^{(\text{KU})}(t),T)$$
$$+ \Gamma^{(\text{MU-F})}(\xi^{(\text{MU})}(t),T) - \Gamma^{(\text{MU-B})}(\xi^{(\text{MU})}(t),T),$$
$$(22a)$$

$$dn_K(t)/dt = -\Gamma^{(\text{KU-F})}(\xi^{(\text{KU})}(t),T) + \Gamma^{(\text{KU-B})}(\xi^{(\text{KU})}(t),T)$$
$$+ \Gamma^{(\text{KT-F})}(\xi^{(\text{KT})}(t),T) - \Gamma^{(\text{KT-B})}(\xi^{(\text{KT})}(t),T),$$
$$(22b)$$

$$dn_p(t)/dt = \Gamma^{(\text{MU-F})}(\xi^{(\text{MU})}(t),T) - \Gamma^{(\text{MU-B})}(\xi^{(\text{MU})}(t),T)$$
$$+ \Gamma^{(\text{KT-F})}(\xi^{(\text{KT})}(t),T) - \Gamma^{(\text{KT-B})}(\xi^{(\text{KT})}(t),T),$$
$$(22c)$$

where $\Gamma^{(\alpha)}$ are the reaction rates ($\alpha = $ KU, MU, KT), and F (B) denotes the forward (backward) process. As a consequence of baryon number conservation, the rate of change of the neutron number density is determined by $dn_p(t)/dt$ through the equation $dn_n(t)/dt = -dn_p(t)/dt$.

---

[6]We do not take into account the structual change of matter associated with a first-order phase transition which may be relevant to a delayed collapse in protonneutron stars. But the first-order phase transition implies that there is a mixed phase where droplets of the kaon-condensed phase are immersed in the normal phase [50]. Recently, it has been pointed out that the existence of the mixed phase has important consequences for the evolution of newly born neutron stars: The scattering of neutrinos off the droplets greatly increases the neutrino opacity [51].

B. Reaction rates

Since the kaon-condensed state is obtained from the underlying chiral symmetry [46], the matrix elements for the relevant reactions can be calculated from the chirally trans-

formed weak Hamiltonian. The expressions for these reaction rates have been given in Paper I [46]. Here we only show the results. For the forward KT process (5a), denoted as KT-F, one obtains

$$\Gamma^{(\text{KT-F})}(\xi^{(\text{KT})},T) = \frac{512}{9(2\pi)^7}\left(g_A G_F \widetilde{f}^2 f \sin\theta_C \cos\theta_C \cos^3\frac{\theta}{2}\frac{|\mathbf{p}_F(n)|^2}{2|\mathbf{p}_F(n)|^2+m_\pi^2}\right)^2 |\mathbf{p}_F(p)|(m_n^*)^3 m_p^* T^5 I^{(\text{KT})}(\xi^{(\text{KT})},T) \quad (23a)$$

$$= (4.0\times10^{30})\left(\frac{|\mathbf{p}_F(p)|}{m_\pi}\right)\left(\frac{m_n^*}{m_N}\right)^3\left(\frac{m_p^*}{m_N}\right)\cos^6\frac{\theta}{2}T_9^5 I^{(\text{KT})}(\xi^{(\text{KT})},T) \quad (\text{cm}^{-3}\,\text{s}^{-1}), \quad (23b)$$

where $\xi^{(\text{KT})}\equiv(\mu_K+\mu_p-\mu_n)/T$ and $I^{(\text{KT})}(u,T)$ is the integral over the kaon momentum divided by T, with $x=|\mathbf{p}_K|/T$:

$$I^{(\text{KT})}(u,T) \equiv \frac{1}{6}\int_0^\infty dx \frac{x^4}{(\widetilde{\omega_-}(x)+\mu_K/T)^3}\frac{(\widetilde{\omega_-}(x)+u)}{1-e^{-\widetilde{\omega_-}(x)}}$$

$$\times\frac{[(\widetilde{\omega_-}(x)+u)^2+4\pi^2]}{e^{\widetilde{\omega_-}(x)+u}-1}, \quad (24)$$

where $\widetilde{\omega_-}(x)\equiv(\omega_-(x)-\mu_K)/T$. In Eq. (23a), $g_A(=1.25)$ is the axial-vector coupling strength, $\widetilde{f}\equiv f_{\pi NN}/m_\pi$ the πNN coupling strength divided by the pion mass, G_F is the Fermi coupling constant, and $\theta_C(\simeq0.24)$ is the Cabibbo angle. The factor $g_A G_F f\sin\theta_C\cos\theta_C\cos^3\theta/2$ originates from a npK^- vertex factor in the transition matrix elements obtained from the chirally rotated hadron currents, whereas the other factor, $\widetilde{f}^2|\mathbf{p}_F(n)|^2/(|\mathbf{p}_F(n)|^2+m_\pi^2)$ with $\mathbf{p}_F(i)$ $(i=n,p)$ the Fermi momentum, comes from the one-pion exchange potential introduced to describe the long-range part of the interactions. Due to the approximate kinematical condition [46], only the nucleon axial-vector current (proportional to g_A) is found to contribute to the KT reactions after all the matrix elements for the lowest-order diagrams are summed. Hence the current for the s-wave condensate, which has only a time component, does not couple to the nonrelativistic nucleon current. The remaining factor in Eq. (23a) arises from the phase space integrals in which m_N^* is the effective nucleon mass and T_9, the temperature in units of 10^9 K. For simplicity, we

take the values of the nucleon effective masses to be $m_p^*/m_N=m_n^*/m_N=0.8$. [36][7]

For the forward KU process (KU-F) [Eq. (3a)], one obtains

$$\Gamma^{(\text{KU-F})}(\xi^{(\text{KU})},T)$$

$$= \frac{G_F^2}{64\pi^5}\sin^2\theta_C\sin^2\theta\{10+3(g_A^2+9\widetilde{g}_A^2)\}$$

$$\times m_N^{*2}\mu_e T^5 I_2(\xi^{(\text{KU})})$$

$$= (6.6\times10^{29})\left(\frac{m_N^*}{m_N}\right)^2\frac{\mu_e}{m_\pi}\sin^2\theta(t)$$

$$\times T_9^5 I_2(\xi^{(\text{KU})})(\text{cm}^{-3}\,\text{s}^{-1}), \quad (25)$$

where $\widetilde{g}_A=F-\frac{1}{3}D=0.15$ with $F+D=g_A=1.25$, $D/(D+F)=0.658$ [21], $I_2(u)\equiv\int_0^\infty dx x^2[\pi^2+(x+u)^2]/[1+\exp(x+u)]$ and $\xi^{(\text{KU})}\equiv(\mu_e-\mu_K)/T$. That the rate for KU-F is proportional to $\sin^2\theta$ is derived from the fact that the

---

[7]Here we have adopted a value for the effective nucleon mass estimated by the nonrelativistic potential models at the saturation density n_0 [36,52]. To be more realistic, the effective nucleon mass varies with the baryon number density. The KT reaction rate depends sensitively on the effective nucleon mass ratio, proportional to $(m_N^*/m_N)^4$, so that, e.g., for a small value of the effective nucleon mass, the production rate of thermal kaons is reduced, and the characteristic time scales for the onset of condensation and equilibration of the system would become long. However, there is a controversy about the density dependence of the effective nucleon mass: In general, the nonrelativistic potential models [52] give a moderate decrease of the effective nucleon mass with density, while the relativistic mean-field models [42,43] give much smaller values than the nonrelativistic potential models at a given density. At a primary stage of our work with regard to the nonequilibrium process of kaon condensation, we would like to emphasize the kinetics of condensation by simplifying the realistic physical situations such as the density dependence of the effective nucleon mass. Hence we assume a constant value $m_N^*/m_N=0.8$ throughout this paper.

matrix element for KU-F is proportional to $\sin\theta$. As a consequence, the KU reactions are operative only when a condensate is present.

For the forward MU process (MU-F) [Eq. (4a)], we refer to Haensel's result [53]:

$$\Gamma^{(\text{MU-F})}(\xi^{(\text{MU})},T)=(5.9\times10^{23})\left(\frac{n_e}{n_0}\right)^{1/3}$$

$$\times\cos^2\frac{\theta}{2}T_9^7J_2(\xi^{(\text{MU})})(\text{cm}^{-3}\,\text{s}^{-1}),$$

(26)

where $J_2(u)\equiv\int_0^\infty dx x^2[9\pi^4+10\pi^2(x+u)^2+(x+u)^4]/[1+\exp(x+u)]$, and $\xi^{(\text{MU})}\equiv(\mu_p+\mu_e-\mu_n)/T$. Here, the matrix elements have been slightly modified by inclusion of an additional factor of $\cos^2(\theta/2)$ due to the presence of a condensate (cf. Paper I).

The backward processes, denoted by the suffix B, are related to the forward processes by way of the following relations:

$$\Gamma^{(\text{KT-B})}(\xi^{(\text{KT})},T)=e^{\xi^{(\text{KT})}}\Gamma^{(\text{KT-F})}(\xi^{(\text{KT})},T),\quad(27)$$

and

$$\Gamma^{(\text{KU-B})}(\xi^{(\text{KU})},T)=\Gamma^{(\text{KU-F})}(-\xi^{(\text{KU})},T),$$

$$\Gamma^{(\text{MU-B})}(\xi^{(\text{MU})},T)=\Gamma^{(\text{MU-F})}(-\xi^{(\text{MU})},T),\quad(28)$$

which are valid at low temperatures [46]. The relation (27) between the forward and backward reaction rates for KT (where bosons are involved) differs from the corresponding relations (28) in the case of the KU or MU process (where only fermions are involved).

C. Initial conditions

We adopt the following initial conditions: At $t=0$, we assume normal neutron-star matter ($\theta=0$), composed of nonrelativistic protons (p), neutrons (n), and ultrarelativistic free electrons (e^-), which is charge neutral, $n_p^0=n_e^0.$[8] The baryon number density n_B for the noncondensed state is taken to be larger than the critical density for kaon condensation, n_B^C ($=3$–$4\,n_0$). Initially, the system is assumed to be in β equilibrium, i.e., $\mu_n^0=\mu_p^0+\mu_e^0$ [$\xi^{(\text{MU})}(t=0)=0$] due to the rapid β-decay reactions, $n\to p+e^-+\bar\nu_e$, $p+e^-\to n+\nu_e$, when the neutron star is hot at an early stage. The initial values for the proton fraction $x_p^0\equiv n_p^0/n_B$ and for the electron chemical potential μ_e^0 are then obtained from the charge neutrality condition, $n_Bx_p^0=(\mu_e^0)^3/(3\pi^2)$, and the β-equilibrium condition where Eq. (12) is used with $\theta=0$. Finally, the total strangeness is assumed to be almost zero corresponding to equal numbers of thermal K^+'s and K^-'s present, which, using Eqs. (14), (17), and (18) with $\theta=0$,

---

[8]The superscript 0 denotes the initial value at $t=0$.

TABLE I. Quantities for the initial noncondensed state ($t=0$) and for the chemically equilibrated state ($t\to\infty$). The former (the latter) quantities are denoted by the superscript 0 (eq). All the values are estimated at $T=0$.

$n_B(\text{fm}^{-3})$	μ_K^0 (MeV)	x_p^0	θ^{eq} (rad)	μ_K^{eq} (MeV)	x_p^{eq}
0.55	-139	0.14	0.48	203	0.23
0.70	-180	0.16	0.91	114	0.39

gives the initial value of the kaon chemical potential $\mu_K^0=-b^0$. As a consequence of these conditions, the initial kaon chemical potential μ_K^0 has a large negative value, while μ_e^0 is positive. Thus the system is far from chemical equilibrium with $|\xi^{(\text{KT})}(t=0)|=|\xi^{(\text{KU})}(t=0)|=|(\mu_e^0-\mu_K^0)/T|\gg1$. For example, one obtains $\xi^{(\text{KT})}(t=0)=-46$ and $\xi^{(\text{KU})}(t=0)=46$ for $\Sigma_{KN}=300$ MeV, $n_B=0.55$ fm^{-3} and $T=1\times10^{11}$ K. Starting from these initial conditions, one can first obtain the number densities $n_i(t)$ at later times from the rate equations (22). Next one can obtain the electron chemical potential $\mu_e(t)$ from the relation $\mu_e(t)=[3\pi^2n_e(t)]^{1/3}$, the kaon chemical potential $\mu_K(t)$ and the chiral angle $\theta(t)$ from Eqs. (15)–(18) and (19), and then the difference between $\mu_p(t)$ and $\mu_n(t)$ from Eq. (12). Because the charge neutrality condition, $n_p(t)=n_K(t)+n_e(t)$, is built into the rate equations (22), it can be seen that this condition is always satisfied. The system evolves dynamically toward an equilibrated kaon-condensed phase through the nonequilibrium weak processes, KU, MU, and KT.

IV. NUMERICAL RESULTS AND DISCUSSION

We choose the value for the KN sigma term to be $\Sigma_{KN}=300$ MeV [54]. The critical density n_B^C is then estimated to be $n_B^C=0.49$ fm^{-3} ($=3.0\,n_0$) (c.f. Ref. [32]). In Table I, we list the values for μ_K^0 and the proton fraction x_p^0 for the initial noncondensed state ($t=0$), and those of θ, μ_K and x_p for the kaon-condensed state in chemical equilibrium ($t\to\infty$) [which we denote by the superscript eq]. It has been shown in Ref. [32] that the temperature dependence of the critical density and physical quantities in the kaon-condensed phase is weak for the temperature less than several tens of MeV. Thus all the values listed in Table I have been estimated at $T=0$. Here, we study the temporal behavior of the physical quantities for two different baryon number densities, $n_B=0.55$ fm^{-3} and 0.70 fm^{-3}. The density $n_B=0.55$ fm^{-3} is close to n_B^C, such that we have a rather weak condensed state with small θ^{eq}. For $n_B=0.70$ fm^{-3}, on the other hand, we have a well-developed condensed state with a large order parameter θ^{eq}. When the baryon number density is increased above the critical density for kaon condensation, the number density of negatively charged kaons increases as the condensate develops. Charge neutrality of the system is maintained by the increase in the proton number density. Consequently, the proton fraction x_p^{eq} increases as the baryon number density increases in an equilibrated kaon-condensed state. On the other hand, the negatively charged electrons are replaced by the negatively charged kaons as a condensate
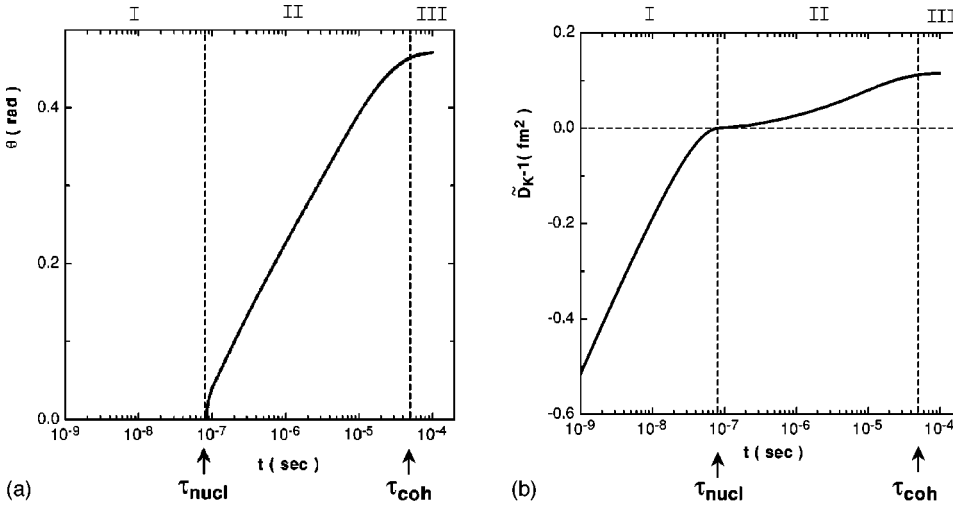
FIG. 1. (a) Chiral angle θ and (b) $\tilde{D}_K^{-1}$, the negative of the expansion coefficient for the thermodynamic potential per unit volume Ω/V with respect to the squared classical kaon field, as a function of time for the baryon number density $n_B = 0.55$ fm^{-3} and the temperature $T = 1.0 \times 10^{11}$ K.

develops with an increase in the baryon number density. The consequent decrease in the electron abundance produces a decrease in the charge chemical potential μ_e^{eq} ($= \mu_K^{eq}$), resulting in a large proton fraction and a reduced charge chemical potential, which are two characteristic features of the kaon-condensed state [2–5].

A. Two typical time scales

In Fig. 1(a), we show the chiral angle θ as a function of time for $n_B = 0.55$ fm^{-3} and $T = 1.0 \times 10^{11}$ K. For the initial values, $\mu_K^0 = -b^0 = -139$ MeV and $x_p^0 = 0.14$. The evolution of the kaon condensate may be divided into the following three stages: (I) no condensate [$\theta(t) = 0$] with thermal kaons present until the onset of condensation, (II) onset of condensation and its monotonic growth, and (III) the asymptotic stage near chemical equilibrium. In equilibrium, one finds $\theta^{eq} = 0.48$ (rad) from Fig. 1(a), and the kaon chemical potential and the proton fraction have the values $\mu_K^{eq} = 203$ MeV and $x_p^{eq} \equiv n_p^{eq}/n_B = 0.23$, respectively, (see Table I).

The onset of condensation from a noncondensed state and its subsequent growth are related to the change in shape of the thermodynamic potential Ω as a function of θ around $\theta = 0$. This change in shape is also associated with the appearance of a soft kaon mode, reflected in a singularity of the distribution function $f_K(\mathbf{p}_K)$, Eq. (18). To see this, we expand $\Omega(t)/V$ around $\theta = 0$:

$$\Omega(t)/V = -\frac{f^2}{2}\tilde{D}_K^{-1}\theta(t)^2 + O(\theta(t)^4),\qquad(29)$$

with

$$\tilde{D}_K^{-1} \equiv D_K^{-1}[\omega = \mu_K(t), \mathbf{p}_K = 0; n_B],$$

where $D_K^{-1}(\omega, \mathbf{p}_K; n_B)$ is the inverse kaon propagator:

$$D_K^{-1}(\omega, \mathbf{p}_K; n_B) \equiv \omega^2 - \mathbf{p}_K^2 + 2b(t)\omega - m_K^{*2}.\qquad(30)$$

Beginning with $\mu_K = -b^0$ at $t = 0$, the kaon chemical potential $\mu_K(t)$ increases monotonically with time. As a result, the

factor $\tilde{D}_K^{-1}$ changes sign, depending on the value of μ_K relative to the critical value, $\mu_K^C(t) \equiv -b(t) + (b(t)^2 + m_K^{*2})^{1/2}$, defined as a root of $\tilde{D}_K^{-1}$. In Fig. 2, we show the thermodynamic potential per particle $\Omega/(Vn_B)$ as a function of θ for $n_B = 0.55$ fm^{-3} and $T = 1.0 \times 10^{11}$ K and the other parameters n_i and μ_i ($i = p, n, e^-, K^-$) fixed at three times corresponding to cases (i)–(iii). Case (i) corresponds to a time before the onset of condensation, for which μ_K is smaller than μ_K^C. [E.g., at $t = 0$, $\mu_K = -b^0 < \mu_K^C$ ($t = 0$).] In this case, $\tilde{D}_K^{-1}$ is negative, which means that the thermodynamic potential per unit volume Ω/V is convex at $\theta = 0$, as seen from Eq. (29) and the curve (i) in Fig. 2, and the noncondensed state ($\theta = 0$) is stable against fluctuations in θ. Because μ_K^C corresponds to the lowest excitation energy of the K^-, $\omega_-(\mathbf{p}_K = 0)$ *in normal matter*, one can see that $\omega_-(\mathbf{p}_K) > \omega_-(\mathbf{p}_K = 0) = \mu_K^C > \mu_K$. Thus the Bose-Einstein distribu-
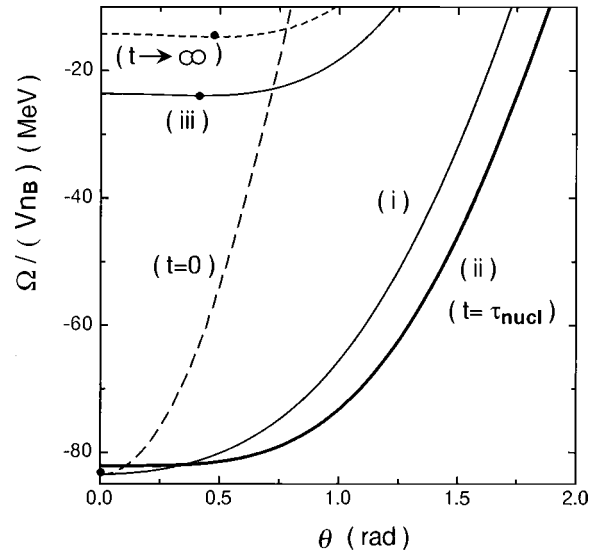

FIG. 2. Thermodynamic potential per particle $\Omega/(Vn_B)$ as a function of θ corresponding to the three cases (i)–(iii). The long-dashed and short-dashed lines correspond to the cases at $t = 0$ and $t \to \infty$, respectively. The dots on the lines represent the locations of the minima of Ω.

tion function f_K here has no singularity. Case (ii) corresponds to a time for which $\mu_K(t) = \mu_K^C(t)$, where $\tilde{D}_K^{-1} = 0$. In this case, the system becomes unstable with respect to the fluctuations in θ [the curve (ii) in Fig. 2], and since $\omega_-(\mathbf{p}_K = 0)(= \mu_K^C)$ is equal to μ_K, $f_K(\mathbf{p}_K)$ becomes divergent at $\mathbf{p}_K = 0$. Thus the appearance of a soft kaon mode with $\omega_-(\mathbf{p}_K = 0) = \mu_K$ implies the onset of an instability due to the formation of a condensate. Finally, case (iii) corresponds to a time after the onset of condensation, for which $\mu_K(t)$ exceeds $\mu_K^C(t)$, so that $\tilde{D}_K^{-1} > 0$. In this case, Ω/V is concave near $\theta = 0$ as a function of θ; which means that the noncondensed state corresponds to the maximum of Ω/V, as seen from the curve (iii) in Fig. 2, and is unstable against the formation of a condensate. The system therefore evolves into a condensate described by $\theta(t)$, which is determined adiabatically by a minimum in the thermodynamic potential [cf. Eq. (19)]. By the use of the dispersion relations for the kaon *in the condensed phase* (see II B) [47], it can be shown that the lowest excitation energy of K^- *in the condensed phase* is equal to μ_K, i.e., $\omega_-(\mathbf{p}_K = 0) = \mu_K(t)$; there is a soft kaon mode in the condensed phase, and $f_K(\mathbf{p}_K)$ is divergent at $\mathbf{p}_K = 0$, as in the case (ii). From Fig. 1(b), where $\tilde{D}_K^{-1}$ is shown as a function of time, one sees that the function $\tilde{D}_K^{-1}$ changes sign at the onset of condensation. We can call the onset time for condensation *the nucleation time*, τ_{nucl}, and the time for growth of the condensate *the coherence time* τ_{coh} after Stoof's discussion about the formation of BEC in an atomic gas [55]. From Fig. 1, one finds $\tau_{\text{nucl}} = 8 \times 10^{-8}$ s, and $\tau_{\text{coh}} = 5 \times 10^{-5}$ s for $n_B = 0.55$ fm^{-3} and $T = 1.0 \times 10^{11}$ K.

B. Connection between the reaction rates and the change in chemical composition

The temporal behavior of the reaction rate for each weak process is shown for $n_B = 0.55$ fm^{-3} and $T = 1.0 \times 10^{11}$ K in Fig. 3. The solid, dashed, and dotted lines denote the KT, MU, and KU processes, respectively. The curves show that the forward thermal kaon process KT-F is dominant in magnitude over the KU and MU reactions throughout the equilibration process [46]. Hence the production of the thermal and condensed kaons proceeds mainly via the KT-F reaction, which is responsible for the onset of condensation and its subsequent growth.

In Fig. 4, we show the temporal behavior of the dimensionless parameters $\xi^{(\alpha)}$ ($\alpha = $ KU, MU, KT), which measure the deviation from chemical equilibrium. Beginning with a large negative value, $\xi^{(\text{KT})}$ increases monotonically toward zero, where the system is in chemical equilibrium with respect to the KT reactions. Note that the KT reaction rates are large even in the initial stage where the system is far from chemical equilibrium ($|\xi^{(\text{KT})}(t)| \gg 1$). In Paper I, we examined in detail the characteristic roles of the soft and hard thermal kaons in the KT reactions, and demonstrated that the high-energy component of the thermal kaons contributes to the KT reaction rates during the noncondensed stage. On the other hand, a low-energy component (a soft mode) of the thermal kaon excitations in the kaon-condensed state was
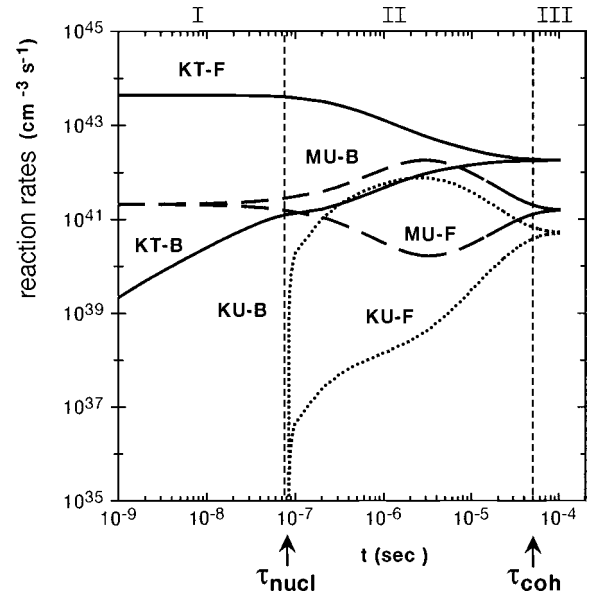

FIG. 3. Temporal behavior of the reaction rates for the weak reactions, KT, KU, and MU for $n_B = 0.55$ fm^{-3} and $T = 1.0 \times 10^{11}$ K.

shown to contribute mainly near chemical equilibrium [46].

Let us now examine how these reactions change the chemical composition. The number densities of the chemical species are shown in Fig. 5 for the same density and temperature as in Figs. 1–4. In stage I ($0 < t < \tau_{\text{nucl}}$), where there is no condensate, the kaons produced by the KT reactions are thermal, and the KU reactions cannot proceed because there is no condensate ($\theta = 0$). The initial β equilibrium is disturbed by the proton excess, created through the KT-F reaction, and the MU reactions are enhanced because the MU-B
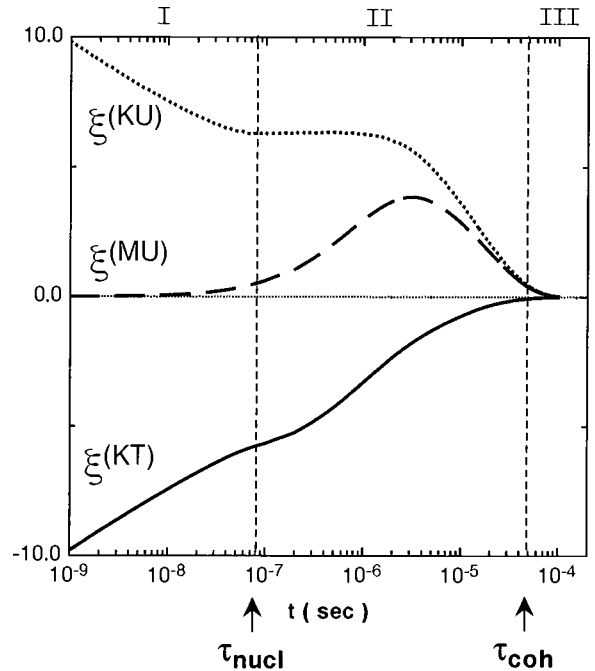

FIG. 4. Temporal behavior of the dimensionless parameters $\xi^{(\alpha)}$ ($\alpha = $ KU, MU, KT) for $n_B = 0.55$ fm^{-3} and $T = 1.0 \times 10^{11}$ K.
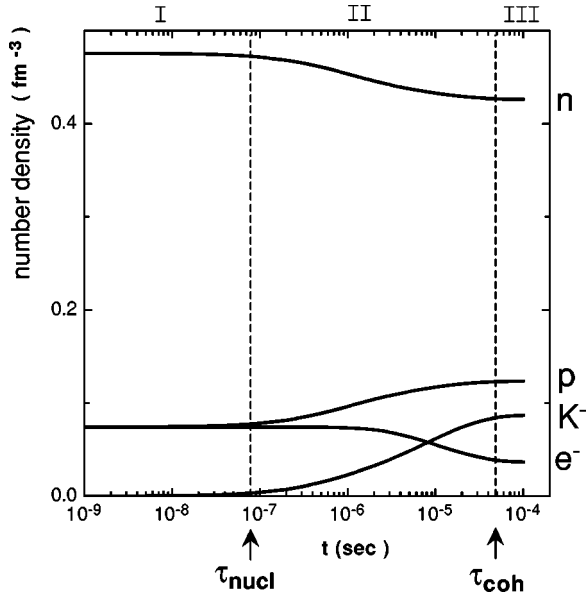
FIG. 5. Temporal behavior of the number densities of the chemical species.

reaction proceeds more rapidly than the MU-F reaction, which restores β equilibrium by reducing the proton excess. Nevertheless, the proton number density n_p still increases, since the KT-F reaction rate is larger than the MU-B reaction rate, as can be seen in Fig. 3 (see also Paper I). Because the total baryon number density n_B is constant, the neutron number density n_n therefore, decreases with time. In stage I, the change in the electron number density n_e is brought about only by the MU reactions, and n_e decreases slightly with time, the MU-B reaction proceeding more rapidly than the MU-F reaction. The extent of the changes in n_p, n_n, and n_e is very small. Consequently, although the electron chemical potential μ_e decreases with time because of the decrease in n_e, this potential, along with the proton and the neutron chemical potentials μ_p and μ_n remain almost constant in stage I. On the other hand, the kaon chemical potential μ_K increases significantly with time; $\mu_K^0 = -b^0$ at $t=0$ and $\mu_K \simeq \mu_K^{eq}$ at $t = \tau_{nucl}$. Hence $\xi^{(KU)}$, which is proportional to $\mu_e - \mu_K$, decreases monotonically with time and $\xi^{(KT)}$ increases monotonically with time (cf. Fig. 4), while $\xi^{(MU)}$ remains close to its initial value (~ 0) except for the time near τ_{nucl}.

In stage II ($\tau_{nucl} < t < \tau_{coh}$), the KU reactions can proceed due to the appearance of a condensate, but the qualitative behavior of each chemical composition is similar to stage I. In particular, the kaon and proton number densities increase through the KT reactions, while those of the electrons and neutrons decrease. The change in the number density of the kaons n_K comes mainly from the condensed part ζ_K [Eq. (15)] after the saturation of the thermal part n_K^T, with the condensed part ζ_K roughly proportional to the square of θ, $\zeta_K \propto \theta^2$, for a small chiral angle, as seen from Eq. (16). According to Fig. 1(a), the chiral angle θ increases rapidly with time for $t \gtrsim \tau_{nucl}$. Thus the change in the number density of the kaons n_K is substantial, being more pronounced in stage II than in stage I due to the appearance of a condensate. The

change in the number density of the electrons n_e in stage II is caused by the KU and MU reactions. But since the reaction rates for the electron absorption processes, KU-B and MU-B, are smaller by orders of magnitude than the rate for the kaon production process KT-F, the change in the number density of the electrons is less marked than the change in the number density of the kaons, and remains almost constant near the onset of condensation, until both the MU-B and KU-B reactions become maximum and operate significantly to reduce n_e in the later part of stage II (cf. Figs. 3 and 5). From the temporal behaviors of n_K, n_e, the charge neutrality, $n_p = n_e + n_K$, and baryon number conservation, $n_p + n_n = n_B$, it can be seen that the change in the number densities of the protons and neutrons become remarkable in stage II.

During the earlier part of stage II where the number density of the electrons is almost constant, the parameter $\xi^{(KU)}$ remains unchanged because both the electron and the kaon chemical potentials are almost constant. On the other hand, as a result of the increase in the proton number density and the decrease in the neutron number density, the difference between the proton and neutron chemical potentials becomes larger with time, as seen from Eq. (12). Thus the parameter $\xi^{(MU)}$ increases with time, after which both $\xi^{(KU)}$ and $\xi^{(MU)}$ decrease with time, and the system enters into the final stage III (cf. Fig. 4).

The coherence time τ_{coh} may be identified with the time at which the magnitudes of the forward and backward reaction rates for KT become equal. As seen in Fig. 3, chemical equilibrium with respect to the KU and MU reactions is achieved at a later time than that at which the KT reaction reaches equilibrium.

Finally, in stage III ($t > \tau_{coh}$), where the system is close to chemical equilibrium ($\xi^{(KT)} \simeq 0$), both the KU and MU reactions compete with each other to determine the dynamical behavior of the system. In this stage, the deviation parameters $\xi^{(KU)}$ and $\xi^{(MU)}$ damp exponentially with time, and the system approaches chemical equilibrium. The relaxation time τ_{rel} can be calculated analytically [see Eq. (A11) in the Appendix]. For $n_B = 0.55$ fm^{-3} and $T = 1.0 \times 10^{11}$ K, the analytic result gives $\tau_{rel} = 2 \times 10^{-4}$ s, which is in agreement with the numerical result read from Fig. 3.

C. Temperature dependence of the characteristic time scales

Next we compare the temperature dependence of the characteristic time scales, τ_{nucl}, τ_{coh}, and τ_{rel} at a fixed baryon number density. Figure 6 shows the behavior of the chiral angle θ for $n_B = 0.55$ fm^{-3} at three different temperatures, $T = 1.0 \times 10^{10}$ K, 1.0×10^{11} K, and 5.0×10^{11} K. In addition, Table II lists the values of τ_{nucl} and τ_{coh}, estimated from the numerical calculations, and the value of τ_{rel}, obtained from Eq. (A11). Roughly speaking, it can be seen that τ_{nucl} depends weakly on temperature, while τ_{coh} and τ_{rel} depend sensitively on temperature: In particular, from Table II and Fig. 6, one obtains $\tau_{nucl} = 2 \times 10^{-8}$ s $\rightarrow 6 \times 10^{-9}$ s, $\tau_{coh} = 2 \times 10^{-1}$ s $\rightarrow 4 \times 10^{-8}$ s, and $\tau_{rel} = 40$ s $\rightarrow 5 \times 10^{-7}$ s as $T = 1.0 \times 10^{10}$ K $\rightarrow 5.0 \times 10^{11}$ K for $n_B = 0.55$ fm^{-3}.
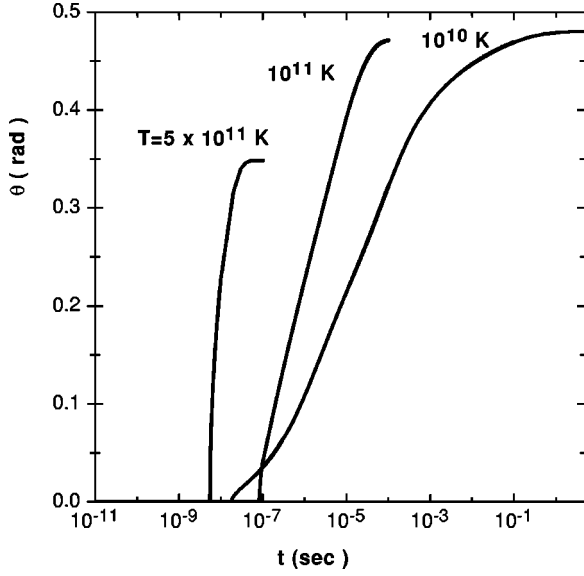
FIG. 6. Temporal behavior of the chiral angle θ for n_B $=0.55$ fm^{-3} and three different temperatures, $T=1.0\times10^{10}$ K, 1.0×10^{11} K, and 5.0×10^{11} K.
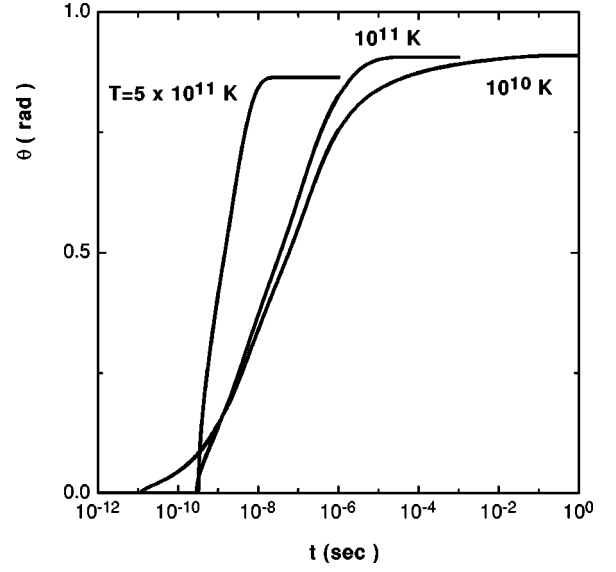

FIG. 7. Temporal behavior of the chiral angle θ for n_B $=0.70$ fm^{-3} and three different temperatures, $T=1.0\times10^{10}$ K, 1.0×10^{11} K, and 5.0×10^{11} K.

Consider first the temperature dependence of the nucleation time, τ_{nucl}, which provides a typical time scale for saturation of the thermal part of the strangeness number density $n_K^T(t)$. For $t>\tau_{\mathrm{nucl}}$, $n_K^T(t)$ changes little. In chemical equilibrium, the thermal kaons occupy a progressively larger part of the total strangeness density as the temperature increases, and two competing effects produce the temperature dependence of τ_{nucl}. (i) The value of $n_K^T(t)$ at saturation is larger at higher temperature, which tends to increase the nucleation time, τ_{nucl}. On the other hand, (ii) a higher temperature gives a higher reaction rate for the relevant KT process. (cf. Paper I). As a consequence the thermal kaon number density $n_K^T(t)$ comes to saturation earlier.

In contrast, the temperature dependence of the coherence time τ_{coh} is explained by the fact that after a condensate appears, its subsequent growth in stage II is controlled mainly by the KT reactions, as seen in Sec. IV B, and the KT reaction rates depend sensitively on the temperature over the entire nonequilibrium processes, (cf. Paper I). This leads to a sensitive temperature dependence of τ_{coh}.

Finally, the relaxation time τ_{rel} depends on the KU and MU reaction rates through the quantities $\tilde{\Gamma}^{\mathrm{(KU\text{-}F)}}$ ($\propto T^5$) and

$\tilde{\Gamma}^{\mathrm{(MU\text{-}F)}}$ ($\propto T^7$) [see Eq. (A9) in Appendix A], and from Eqs. (A11) and (A9), it can be seen that the relaxation time τ_{rel} depends sensitively on the temperature, so as to decrease significantly as the temperature increases.

D. Density-dependence of the characteristic time scales

Here we discuss the temporal behavior of the system at a higher baryon number density, $n_B=0.70$ fm^{-3}, for which one can expect a fully developed kaon-condensed phase when the system is in chemical equilibrium. Initially we start with $n_K^T(t=0)=0$, which gives $\mu_K^0=-b^0=-180$ MeV and $x_p^0=0.16$. The temporal behavior of the chiral angle θ is shown in Fig. 7 for $n_B=0.70$ fm^{-3} for the same three temperatures as in Fig. 6. The numerical values for the nucleation time τ_{nucl}, the coherence time τ_{coh}, and the relaxation time τ_{rel} for the density and temperatures corresponding to the three curves shown are listed in Table II. From an examination of this table and Fig. 7, it can be seen that while the nucleation time τ_{nucl} depends weakly on the temperature, the coherence time τ_{coh} and the relaxation time τ_{rel} depend sensitively on the temperature, becoming shorter as the temperature is raised. These features for τ_{nucl}, τ_{coh}, and τ_{rel} are qualitatively the same as in the case of the lower baryon number density $n_B=0.55$ fm^{-3}.

The time scales obtained for $n_B=0.70$ fm^{-3} can be compared with those for $n_B=0.55$ fm^{-3}. From Table II, one can see that the nucleation time τ_{nucl} is sensitive to the baryon number density, with the ratio τ_{nucl} $(0.55$ fm$^{-3})/\tau_{\mathrm{nucl}}$ $(0.70$ fm$^{-3})$ equal to 2×10 -2×10^3 for 1×10^{10} K$<T<5\times10^{11}$ K. This density dependence is explained as follows: In the noncondensed state where $|\xi^{\mathrm{(KT)}}|\gg1$ ($\xi^{\mathrm{(KT)}}<0$), the KT-F reaction rate is very sensitive to $|\xi^{\mathrm{(KT)}}|$ and becomes large rapidly as $|\xi^{\mathrm{(KT)}}|$ increases [46]. In addition, the kaon chemical potential μ_K (<0 at $t=0$) in $|\xi^{\mathrm{(KT)}}|$ increases rapidly with time in stage I,

TABLE II. The nucleation time τ_{nucl}, the coherence time τ_{coh}, and the relaxation time τ_{rel} for different densities and temperatures.

n_B(fm^{-3})	T (K)	τ_{nucl} (s)	τ_{coh} (s)	τ_{rel} (s)
0.55	1×10^{10}	2×10^{-8}	2×10^{-1}	4×10
	1×10^{11}	8×10^{-8}	5×10^{-5}	2×10^{-4}
	5×10^{11}	6×10^{-9}	4×10^{-8}	5×10^{-7}
0.70	1×10^{10}	1×10^{-11}	6×10^{-2}	9×10
	1×10^{11}	3×10^{-10}	1×10^{-5}	2×10^{-4}
	5×10^{11}	3×10^{-10}	2×10^{-8}	1×10^{-7}

and, before the onset of condensation, it is already almost equal to the equilibrium value μ_K^{eq} (>0), which has a smaller value for a larger baryon number density. As compared with the density dependence of μ_K, the density dependence of the difference between the proton and neutron chemical potentials $\mu_p - \mu_n$ (<0) in $|\xi^{(\mathrm{KT})}|$ is weak. Hence, as the baryon number density increases, the parameter $|\xi^{(\mathrm{KT})}|$ ($= |\mu_K + \mu_p - \mu_n|/T \gg 1$) increases mainly due to the decrease in μ_K. As a result, the KT-F reaction rate in stage I is much larger for a larger baryon number density, which considerably reduces the time required for saturation of the thermal kaon number density.

After the appearance of a condensate, the value of $|\xi^{(\mathrm{KT})}|$ becomes sufficiently small, so that the density dependence of $|\xi^{(\mathrm{KT})}|$ becomes insignificant. Therefore, the KT-F reaction rate does not depend much on n_B. Hence the coherence time τ_{coh}, which is controlled by the KT-F reaction, shows only a weak dependence on n_B. In a similar way, near chemical equilibrium where $|\xi^{(\mathrm{KU})}| \ll 1$ and $|\xi^{(\mathrm{MU})}| \ll 1$, the density dependence of both the KU-F and MU-F reaction rates is weak, and therefore τ_{rel}, which is determined by these reaction rates, is found to have a weak dependence on n_B.

E. Implications for the delayed collapse of a protoneutron star

From Table II, one can see that a condensate develops fully with a characteristic time scale given by the coherence time τ_{coh}. In the context of the delayed collapse of a newly born neutron star, we consider some implications of the results. Since the neutrino degeneracy is not taken into account in our framework, our results are applicable to the cooling era after the deleptonization. Hence the delayed collapse associated with a kaon condensate should be considered in this cooling era.

The low temperature case (e.g., $T = 1 \times 10^{10}$ K) may apply to the final stage of the cooling era, while the high temperature case (e.g., $T \gtrsim 10^{11}$ K) to the initial stage. In both cases, we have found that the time scale of τ_{coh} is very small; $\tau_{\mathrm{coh}} \sim 0.1$ s for $T = 1 \times 10^{10}$ K and $\tau_{\mathrm{coh}} \lesssim 5 \times 10^{-5}$ s for $T \gtrsim 10^{11}$ K, which should be compared with the cooling time scale of the order of 10 s. Hence we can conclude that, in both cases, the time delay of a collapse due to the formation of a condensate is negligible as compared with the cooling time scale and will have a minor effect on the evolution of the protoneutron star.

V. SUMMARY AND CONCLUDING REMARKS

We have considered the kinetics of kaon condensation by the use of rate equations which include the three weak reactions: the thermal kaon process, the kaon-induced Urca process, and the modified Urca process. The thermal kaon process is shown to be dominant over other weak reactions throughout the equilibration process. The evolution of the kaon condensate is divided into the following three stages: (I) the noncondensed stage before the onset of condensation, (II) onset of condensation and its growth until its saturation, and (III) the asymptotic relaxation stage near chemical equilibrium. The role of thermal kaons and especially the con-

nection between the existence of a soft kaon mode and the instability of the noncondensed state has been clarified. It has been found that a full development of a condensate is characterized by a time scale given by the coherence time τ_{coh}. Using these results, we have made a brief comment on implications of our results on the delayed collapse mechanism of a newly born neutron star into a black hole. The situation adopted in our framework may be applicable to the cooling era after the deleptonization. It is found that the time scale of the development of a condensate (the coherence time) is much smaller than that of the cooling for the relevant temperatures (1 MeV– several tens of MeV). Therefore, the time delay for the formation of a kaon condensate may not affect the delayed collapse of a neutron star.

Several effects which should be taken into account within our framework in the future are as follows:

(1) We have used the thermodynamic potential neglecting any fluctuations except for those produced by thermal kaons. However, for a neutron star just born in a supernova, since the initial temperature is as high as several tens of MeV, thermal fluctuations other than the kaon thermal loop contributions [47] should be fully incorporated into the thermodynamic potential.

(2) Furthermore, since the matter is opaque to the neutrinos at high temperatures, the thermal effects associated with neutrino diffusion may also be important. In particular, the degenerate neutrinos will contribute to the thermodynamic potential and influence the relevant reaction rates. Therefore, the neutrino diffusion may affect the thermal evolution of a newly-born neutron star.

(3) The reaction rates for the relevant weak processes have been obtained in the low temperature approximation (cf Paper I). The expressions for the reaction rates must be extended to the high temperature case, and the phase-space integrals should be performed numerically beyond the low temperature approximation [56].

(4) During the equilibration process, we have assumed that the temperature T is constant: the energy produced by the weak reactions is lost to the surroundings. However, because the energy release due to the nonequilibrium weak reactions will heat up the matter, the temperature is in general time-dependent during the course of the equilibration process, and this can affect the evolution of the star. This thermal effect can be included through an additional equation that determines the rate of change of the internal energy of the system.[9] A significant increase in the temperature could possibly lead to further reduction of the time scale for the growth of a condensate represented by the coherence time. On the other hand, as a result of the raise in the temperature, the critical density n_B^C for kaon condensation can be

---

[9] In Ref. [56], strangeness production in quark matter has been considered with allowance for the time dependence of the temperature. It has been shown that the temperature changes appreciably with time up to ~ 50 MeV during the nonequilibrium process, and that the time scale for saturation of the strangeness in this case is smaller by orders of magnitude than the case where the temperature is held fixed.

pushed up to higher density, which may cause the delay in the onset of condensation. In this respect, it is necessary to obtain a phase diagram in the $T-n_B$ plane [47,32], and the dynamics of the onset and growth of condensation must be considered along a trajectory in this plane.

APPENDIX: ASYMPTOTIC BEHAVIOR NEAR CHEMICAL EQUILIBRIUM

We derive an expression for the relaxation time which characterizes the asymptotic behavior of the system near chemical equilibrium (stage III).

1. Linearization of $\xi^{(KU)}(t)$ and $\xi^{(MU)}(t)$

In stage III, both the forward and backward KT reaction rates are almost equal, i.e., $\xi^{(KT)}(t) \simeq 0$. Therefore, we consider the case where the relaxation proceeds only through the KU and MU reactions, neglecting the KT reaction. The parameters $\xi^{(KU)}(t)$ and $\xi^{(MU)}(t)$ are written as

$$\xi^{(KU)}(t) = [\delta\mu_e(t) - \delta\mu_K(t)]/T, \tag{A1a}$$

$$\xi^{(MU)}(t) = [\delta\mu_e(t) + \delta\mu_p(t) - \delta\mu_n(t)]/T, \tag{A1b}$$

where $\delta\mu_i(t)$ $(i = p, n, e^-, K^-)$ is the deviation of the chemical potential from the equilibrium value, i.e., $\delta\mu_i(t) = \mu_i(t) - \mu_i^{eq}$. From the relation, $\mu_e = (3\pi^2 n_e)^{1/3}$, one obtains

$$\delta\mu_e(t) = (\pi/\mu_e^{eq})^2 \delta n_e(t), \tag{A2}$$

where $\delta n_e(t) = n_e(t) - n_e^{eq}$. One can also write the deviations of the chemical potentials $\delta\mu_K(t)$ and $\delta\mu_p(t) - \delta\mu_n(t)$ in terms of $\delta n_i(t)$ $(= n_i(t) - n_i^{eq})$ from linearized forms of the three equations with respect to $\delta\mu_K(t)$, $\delta\theta(t)$, $\delta\mu_p(t) - \delta\mu_n(t)$, and $\delta n_i(t)$ represented by the expression for the kaon number density [Eq. (15)], the classical field equation [Eq. (19)], and the expression for the difference between μ_p and μ_n [Eq. (12)]. Note that we can neglect the deviation of the thermal kaon part in the kaon number density, i.e., $\delta n_K(t) = \delta\zeta_K(t)$ $[\delta n_K^T(t) = 0]$, because the thermal kaon number density $n_K^T(t)$ is almost constant after a condensate appears until the system reaches chemical equilibrium.

The deviation of the electron number density $\delta n_e(t)$ is divided into two contributions:

$$\delta n_e(t) = \delta^{(KU)} n_e(t) + \delta^{(MU)} n_e(t), \tag{A3}$$

where $\delta^{(KU)} n_e(t)$ $[\delta^{(MU)} n_e(t)]$ is caused by the KU reactions (the MU reactions). The number densities for the other species are related to $\delta^{(KU)} n_e(t)$ and $\delta^{(MU)} n_e(t)$ by

$$\delta n_K(t) = -\delta^{(KU)} n_e(t), \tag{A4a}$$

$$\delta n_p(t) = \delta^{(MU)} n_e(t), \tag{A4b}$$

$$\delta n_n(t) = -\delta n_p(t) = -\delta^{(MU)} n_e(t). \tag{A4c}$$

Following the above results, the deviation parameters (A1) can be expressed in terms of $\delta^{(KU)} n_e(t)$ and $\delta^{(MU)} n_e(t)$. The result is

$$\xi^{(KU)}(t) = \frac{p}{T}\delta^{(KU)} n_e(t) + \frac{q}{T}\delta^{(MU)} n_e(t), \tag{A5a}$$

$$\xi^{(MU)}(t) = \frac{q}{T}\delta^{(KU)} n_e(t) + \frac{r}{T}\delta^{(MU)} n_e(t), \tag{A5b}$$

where

$$p = \left[\left(\frac{\pi}{\mu_e}\right)^2 + \frac{1}{f^2\{\sin^2\theta + 4(\cos\theta + b/\mu_K)^2\}}\right]^{eq}, \tag{A6a}$$

$$q = \left[\left(\frac{\pi}{\mu_e}\right)^2 + \frac{1 + \cos\theta + 2b/\mu_K}{2f^2\{\sin^2\theta + 4(\cos\theta + b/\mu_K)^2\}}\right]^{eq}, \tag{A6b}$$

$$\begin{aligned} r = \Bigg[&\left(\frac{\pi}{\mu_e}\right)^2 + \frac{(1 - \cos\theta)(\cos\theta + 2b/\mu_K)}{2f^2\{\sin^2\theta + 4(\cos\theta + b/\mu_K)^2\}} \\ &+ \frac{2}{3}\frac{(3\pi^2)^{2/3}}{2m_N}(n_p^{-1/3} + n_n^{-1/3}) + \frac{8V_{sym}(n_B)}{n_B}\Bigg]^{eq}. \end{aligned} \tag{A6c}$$

In Eq. (A6), the first term comes from the deviation of the electron chemical potential $\delta\mu_e$, Eq. (A2), and the second term from the deviation of the parameters for a condensate, i.e., $\delta\mu_K$ and $\delta\theta$. The third and fourth terms in Eq. (A6c) come from the deviation of the proton and neutron chemical potentials. It is to be noted that a condensate already develops fully in stage III, so that the quantities for the condensate are almost constant. Thus it is a good approximation to set $\delta\mu_K = \delta\theta = 0$, which leads to $p = q \simeq (\pi/\mu_e^{eq})^2$, and

$$r \simeq \left[\left(\frac{\pi}{\mu_e}\right)^2 + \frac{2}{3}\frac{(3\pi^2)^{2/3}}{2m_N}(n_p^{-1/3} + n_n^{-1/3}) + \frac{8V_{sym}(n_B)}{n_B}\right]^{eq}.$$

2. Differential equations for $\xi^{(KU)}(t)$ and $\xi^{(MU)}(t)$

By differentiating both sides of Eq. (A5) with time, one finds that the rates of change of $\xi^{(KU)}(t)$ and $\xi^{(MU)}(t)$ are related to the reaction rates for KU and MU, through the rate equations

$$\frac{d}{dt}\delta^{(\text{KU})}n_e(t)=\Gamma^{(\text{KU-F})}(\xi^{(\text{KU})}(t),T)-\Gamma^{(\text{KU-F})}(-\xi^{(\text{KU})}(t),T),$$
(A7a)

$$\frac{d}{dt}\delta^{(\text{MU})}n_e(t)=\Gamma^{(\text{MU-F})}(\xi^{(\text{MU})}(t),T)-\Gamma^{(\text{MU-F})}(-\xi^{(\text{MU})}(t),T).$$
(A7b)

For the system close to chemical equilibrium, $|\xi^{(\text{KU})}(t)|\ll1$ and $|\xi^{(\text{MU})}(t)|\ll1$. In this case, the rhs of Eqs. (A7a) and (A7b) can be expanded up to first order in $\xi^{(\text{KU})}(t)$ and $\xi^{(\text{MU})}(t)$, respectively. Thus one obtains the coupled differential equations for $\xi^{(\text{KU})}(t)$ and $\xi^{(\text{MU})}(t)$:

$$\frac{d}{dt}\xi^{(\text{KU})}(t)=-\frac{p}{T}\tilde{\Gamma}^{(\text{KU-F})}\cdot\xi^{(\text{KU})}(t)-\frac{q}{T}\tilde{\Gamma}^{(\text{MU-F})}\cdot\xi^{(\text{MU})}(t),$$
(A8a)

$$\frac{d}{dt}\xi^{(\text{MU})}(t)=-\frac{q}{T}\tilde{\Gamma}^{(\text{KU-F})}\cdot\xi^{(\text{KU})}(t)-\frac{r}{T}\tilde{\Gamma}^{(\text{MU-F})}\cdot\xi^{(\text{MU})}(t),$$
(A8b)

where

$$\tilde{\Gamma}^{(\text{KU-F})}\equiv2\frac{|I_2'(0)|}{I_2(0)}\Gamma^{(\text{KU-F})}(\xi^{(\text{KU})}=0,T)$$

$$\simeq1.3\times\Gamma^{(\text{KU-F})}(\xi^{(\text{KU})}=0,T)\propto T^5,\quad\text{(A9a)}$$

$$\tilde{\Gamma}^{(\text{MU-F})}\equiv2\frac{|J_2'(0)|}{J_2(0)}\Gamma^{(\text{MU-F})}(\xi^{(\text{MU})}=0,T)$$

$$\simeq1.2\times\Gamma^{(\text{MU-F})}(\xi^{(\text{MU})}=0,T)\propto T^7,\quad\text{(A9b)}$$

with $I_2(0)=\frac{3}{2}\pi^2\zeta(3)+\frac{45}{2}\zeta(5)=41.13$,

$$I_2'(0)\equiv(dI_2(u)/du)_{u=0}=-\frac{17}{60}\pi^4,$$

$$J_2(0)=\frac{27}{2}\pi^4\zeta(3)+225\pi^2\zeta(5)+\frac{2835}{4}\zeta(7)=4598,$$

and

$$J_2'(0)\equiv(dJ_2(u)/du)_{u=0}=-\frac{367}{126}\pi^6.$$

From Eq. (A8), one obtains the following forms of the solutions:

$$\xi^{(\text{KU})}(t)=C_1e^{-t/\tau_a}+C_2e^{-t/\tau_b},\quad\text{(A10a)}$$

$$\xi^{(\text{MU})}(t)=C_3e^{-t/\tau_a}+C_4e^{-t/\tau_b},\quad\text{(A10b)}$$

where C_1-C_4 are constants, and τ_a and τ_b are time constants which characterize the asymptotic evolution of the system. The relaxation time τ_{rel} is defined as the larger of τ_a and τ_b, and one obtains

$$\tau_{\text{rel}}=\frac{T}{2}\frac{p\tilde{\Gamma}^{(\text{KU-F})}+r\tilde{\Gamma}^{(\text{MU-F})}+[\{p\tilde{\Gamma}^{(\text{KU-F})}-r\tilde{\Gamma}^{(\text{MU-F})}\}^2+4q^2\tilde{\Gamma}^{(\text{KU-F})}\tilde{\Gamma}^{(\text{MU-F})}]^{1/2}}{(pr-q^2)\tilde{\Gamma}^{(\text{KU-F})}\tilde{\Gamma}^{(\text{MU-F})}}.$$
(A11)

[1] D. B. Kaplan and A. E. Nelson, Phys. Lett. B **175**, 57 (1986); **179**, 409(E) (1986); A. E. Nelson and D. B. Kaplan, *ibid.* **192**, 193 (1987).

[2] For a review, T. Tatsumi, Prog. Theor. Phys. Suppl. **120**, 111 (1995).

[3] H. Fujii, T. Maruyama, T. Muto, and T. Tatsumi, Nucl. Phys. **A597**, 645 (1996).

[4] C. -H. Lee, Phys. Rep. **275**, 197 (1996).

[5] M. Prakash, I. Bombaci, M. Prakash, P. J. Ellis, J. M. Lattimer, and R. Knorren, Phys. Rep. **280**, 1 (1997).

[6] G. E. Brown, C.- H. Lee, and R. Rapp, Nucl. Phys. **A639**, 455c (1998).

[7] V. Koch, Phys. Lett. B **337**, 7 (1994).

[8] T. Waas, N. Kaiser, and W. Weise, Phys. Lett. B **365**, 12 (1996); **379**, 34 (1996); T. Waas and W. Weise, Nucl. Phys. **A625**, 287 (1997).

[9] M. Lutz, Phys. Lett. B **426**, 12 (1998).

[10] C. J. Batty, E. Friedman, and A. Gal, Phys. Rep. **287**, 385 (1997).

[11] J. Schaffner-Bielich, I. N. Mishustin, and J. Bondorf, Nucl. Phys. **A625**, 325 (1997).

[12] G. Q. Li, C.- H. Lee, and G. E. Brown, Phys. Rev. Lett. **79**, 5214 (1997); Nucl. Phys. **A625**, 372 (1997).

[13] W. Cassing and E. L. Bratkowskaya, Phys. Rep. **308**, 65 (1999).

[14] For a review, P. Senger and H. Ströbele, J. Phys. G **25**, R59 (1999).

[15] G. Song, B.- A. Li, and C. M. Ko, Nucl. Phys. **A646**, 481 (1999).

[16] J. Schaffner-Bielich, V. Koch, and M. Effenberger, report LBNL-41395 (nucl-th/9907095).

[17] V. Thorsson, M. Prakash, and J. M. Lattimer, Nucl. Phys. **A572**, 693 (1994); **A574**, 851(E) (1994).

[18] G. E. Brown, K. Kubodera, D. Page, and P. Pizzecherro, Phys. Rev. D **37**, 2042 (1988).

[19] T. Tatsumi, Prog. Theor. Phys. **80**, 22 (1988).

[20] D. Page and E. Baron, Astrophys. J. Lett. **354**, L17 (1990).

[21] H. Fujii, T. Muto, T. Tatsumi, and R. Tamagaki, Nucl. Phys. **A571**, 758 (1994); Phys. Rev. C **50**, 3140 (1994).

[22] G. E. Brown and H. A. Bethe, Astrophys. J. **423**, 659 (1994).

[23] T. W. Baumgarte, S. L. Shapiro, and S. Teukolsky, Astrophys. J. **443**, 717 (1995); **458**, 680 (1996).

[24] T. Harada, K. Nakano, T. Tatsumi, and M. Yasuhira (in preparation).

[25] T. Takatsuka, Prog. Theor. Phys. **80**, 361 (1988); **82**, 475 (1989); in *The Structure and Evolution of Neutron Stars, Kyoto, 1990*, edited by D. Pines, R. Tamagaki, and S. Tsuruta (Addison-Wesley, Redwood City, CA, 1992), p. 257.

[26] M. Takahara and K. Sato, Prog. Theor. Phys. **80**, 861 (1988).

[27] N. K. Glendenning, Astrophys. J. **448**, 797 (1995).

[28] W. Keil and H.-Th. Janka, Astron. Astrophys. **296**, 145 (1995).

[29] J. A. Pons *et al.*, Astrophys. J. **513**, 780 (1999).

[30] O. G. Benvenuto and J. E. Horvath, Phys. Rev. Lett. **63**, 716 (1989).

[31] M. Prakash, J. Cooke, and J. M. Lattimer, Phys. Rev. D **52**, 661 (1995).

[32] M. Yasuhira and T. Tatsumi, Proceedings of PANIC 99 (KUNS-1589), nucl-th/9908064.

[33] A. Akmal, V. R. Pandharipande, and D. G. Ravenhall, Phys. Rev. C **58**, 1804 (1998).

[34] J. W. Percival *et al.*, Astrophys. J. **446**, 832 (1995).

[35] T. Muto, T. Tatsumi, and N. Iwamoto, Aust. J. Phys. **50**, 13 (1997).

[36] B. L. Friman and O. V. Maxwell, Astrophys. J. **232**, 541 (1979).

[37] O. V. Maxwell, Astrophys. J. **316**, 691 (1987).

[38] J. Boguta, Phys. Lett. **106B**, 255 (1981).

[39] J. M. Lattimer, C. J. Pethick, M. Prakash, and P. Haensel, Phys. Rev. Lett. **66**, 2701 (1991).

[40] M. Prakash, M. Prakash, J. M. Lattimer, and C. J. Pethick, Astrophys. J. Lett. **390**, L77 (1992).

[41] N. K. Glendenning, Astrophys. J. **293**, 470 (1985); Phys. Rev. Lett. **81**, 2176 (1998), and references therein.

[42] P. J. Ellis, R. Knorren, and M. Prakash, Phys. Lett. B **349**, 11 (1995); R. Knorren, M. Prakash, and P. J. Ellis, Phys. Rev. C **52**, 3470 (1995).

[43] J. Schaffner and I. Mishustin, Phys. Rev. C **53**, 1416 (1996).

[44] S. Balberg and A. Gal, Nucl. Phys. **A625**, 435 (1997).

[45] M. Baldo, G. F. Burgio, and H. -J. Schulze, Phys. Rev. C **58**, 3688 (1998).

[46] T. Muto, T. Tatsumi, and N. Iwamoto, Phys. Rev. D **61**, 063001 (2000), Paper I.

[47] T. Tatsumi, *Proceedings of the APCTP workshop on Astrohadron physics*, edited by G. E. Brown *et al.* (World Scientific, Singapore, 1999), p. 594; T. Tatsumi and M. Yasuhira, Phys. Lett. B **441**, 9 (1998); Nucl. Phys. **A653**, 133 (1999); nucl-th/9904038.

[48] M. Prakash, T. L. Ainsworth, and J. M. Lattimer, Phys. Rev. Lett. **61**, 2518 (1988).

[49] V. Thorsson and P. J. Ellis, Phys. Rev. D **55**, 5177 (1997).

[50] N. K. Glendenning and J. Schaffner-Bielich, Phys. Rev. Lett. **81**, 4564 (1998); Phys. Rev. C **60**, 025803 (1999).

[51] S. Reddy, G. Bertsch, and M. Prakash, nucl-th/9909040.

[52] R. B. Wiringa, V. Fiks, and A. Fabrocini, Phys. Rev. C **38**, 1010 (1988).

[53] P. Haensel, Astron. Astrophys. **262**, 131 (1992).

[54] J. F. Donoghue and C. R. Nappi, Phys. Lett. **168B**, 105 (1986); R. L. Jaffe and C. L. Korpa, Comments Nucl. Part. Phys. **17**, 163 (1987).

[55] H. T. C. Stoof, in *Bose-Einstein Condensation*, edited by A. Griffin, D. W. Snoke, and S. Stringari (Cambridge University Press, Cambridge, England, 1995), p. 226.

[56] S. K. Ghosh, S. C. Phatak, and P. K. Sahu, Nucl. Phys. **A596**, 670 (1996).